Human Immunoglobulin Adsorption Investigated by Means of Quartz Crystal Microbalance Dissipation, Atomic Force Microscopy, Surface Acoustic Wave, and Surface Plasmon Resonance Techniques

Cheng Zhou,*,†,‡ Jean-Michel Friedt,† Angelina Angelova,† Kang-Hoon Choi,† Wim Laureyn,† Filip Frederix,† Laurent A. Francis,†,§ Andrew Campitelli,† Yves Engelborghs,‡ and Gustaaf Borghs†

Biosensors group, Interuniversity Microelectronics Center (IMEC), Kapeldreef 75, 3001 Leuven, Belgium, Laboratory of Biomolecular Dynamic, Department of Chemistry KULeuven, Celestijnenlaan 200D, 3001 Leuven, Belgium, PCPM, Université catholique de Louvain, Croix du Sud 1, 1348 Louvain-la-Neuve, Belgium

Received December 1, 2003. In Final Form: March 12, 2004

Time-resolved adsorption behavior of a human immunoglobin G (hIgG) protein on a hydrophobized gold surface is investigated using multitechniques: quartz crystal microbalance/dissipation (QCM-D) technique; combined surface plasmon resonance (SPR) and Love mode surface acoustic wave (SAW) technique; combined QCM-D and atomic force microscopy (AFM) technique. The adsorbed hIgG forms interfacial structures varying in organization from a submonolayer to a multilayer. An "end-on" IgG orientation in the monolayer film, associated with the surface coverage results, does not corroborate with the effective protein thickness determined from SPR/SAW measurements. This inconsistence is interpreted by a deformation effect induced by conformation change. This conformation change is confirmed by QCM-D measurement. Combined SPR/SAW measurements suggest that the adsorbed protein barely contains water after extended contact with the hydrophobic surface. This limited interfacial hydration also contributed to a continuous conformation change in the adsorbed protein layer. The viscoelastic variation associated with interfacial conformation changes induces about 1.5 times overestimation of the mass uptake in the QCM-D measurements. The merit of combined multitechnique measurements is demonstrated.

Introduction

Adsorption of immunoglobin G (IgG) on solid surfaces has attracted strong research interest because of its wide application in biotechnology, immunoassays, and biosensors.[1−4] The detailed understanding of the mechanisms and physicochemical parameters governing the adsorption behavior is essential for the development of novel immunoassays and biosensors. Various techniques, based on different principles such as radiolabeling,[5−7] optical adsorption,[8−10] refractive index changes,[11−18] electromechanical microbalance,[4,19,20] and others,[21−28] have been used to investigate IgG adsorption.

However, the adsorption of IgG macromolecules at the liquid−solid interface is a sophisticated process.[9,10,14,16,22,24,28−30] The understanding of the mechanisms of the IgG adsorption should be improved by the simultaneous investigation of the protein film properties, such

* To whom correspondence may be addressed. Phone: +32 16 288600. Fax: +32 16 281097. E-mail: Cheng.zhou@imec.be.
† Biosensors group, Interuniversity Microelectronics.
‡ Department of Chemistry, KULeuven.
§ PCMP, Universite catholique de Louvain.

(1) Sevier, E. D. *J. Med. Technol.* **1985**, *2*, 287−293.
(2) Guesdon J. L.; Avrameas S. In *Applied Biochemistry and Bioengineering*; Wingard L. B., Katchalski-katzir E., Goldstein L., Eds.; Academic Press: New York, 1981, Vol. 3, p 207.
(3) Buijs, J.; Lichtenbelt, J. W. T.; Norde, W.; Lyklema, J. *Colloids Surf., B* **1995**, *5*, 11−23.
(4) Caruso, F.; Niikura, K.; Furlong, D. N.; Okahata, Y. *Langmuir* **1997**, *13*, 3427−3433.
(5) Wagner, M. S.; Horbett, T. A.; Castner, D. G. *Langmuir* **2003**, *19*, 1708−1715.
(6) Moulton, S. E.; Barisci, J. N.; Bath, A.; Stella, R.; Wallace, G. G. *J. Colloid Interface Sci.* **2003**, *261*, 312−319.
(7) Baszkin, A.; Boissonnade, M. M.; Kamyshny, A.; Magdassi, S. *J. Colloid Interface Sci.* **2001**, *244*, 18−23.
(8) Buijs, J.; Norde, W. *Langmuir* **1996**, *12*, 1605−1613.
(9) Moulton, S. E.; Barisci, J. N.; McQuillan, A. J.; Wallace, G. G. *Colloids Surf., A* **2003**, *220*, 159−167.
(10) Giacomelli, C. E.; Bremer, M. G. E. G.; Norde, W. *J. Colloid Interface Sci.* **1999**, *220*, 13−23.
(11) Green, R. J.; Davies, J.; Davies, M. C.; Roberts, C. J.; Tendler, S. J. B. *Biomaterials* **1997**, *18*, 405−413.
(12) Green, R. J.; Davies, M. C.; Roberts, C. J.; Tendler, S. J. B. *Biomaterials* **1999**, *20*, 385−391
(13) Petrash, S.; Cregger, T.; Zhou, B.; Pokidysheva, E.; Foster, M. D.; Brittain, W. J.; Sevastianov, V.; Majkrzak, C. F. *Langmuir* **2001**, *17*, 7645−7651.
(14) Buijs, J.; Van Den Berg, P. A. W.; Lichtenbelt, J. W. T.; Norde, W.; Lyklema J. *J. Colloid Interface Sci.* **1996**, *178*, 594−605.
(15) Lassen, B.; Malmsten, M. *J. Colloid Interface Sci.* **1996**, *180*, 339−349.
(16) Malmsten, M. *Colloids Surf., B* **1995**, *3*, 297−308.
(17) Malmsten, M. *J. Colloid Interface Sci.* **1995**, *172*, 106−115.
(18) Heinrich, L.; Mann, E. K.; Voegel, J. C.; Koper, G. J. M.; Schaaf, P. *Langmuir* **1996**, *12*, 4857−4865.
(19) Marxer, C. G.; Coen, M. C.; Schlapbach, L. *J. Colloid Interface Sci.* **2003**, *261*, 291−298.
(20) Otzen, D. E.; Oliveberg, M.; Höök F. *Colloids and Surf., B* **2003**, *29*, 67−73.
(21) Kamyshny, A.; Lagerge, S.; Partyka, S.; Relkin, P.; Magdassi, S. *Langmuir* **2001**, *17*, 8242−8248.
(22) Vermeer, A. W. P.; Giacomelli, C. E.; Norde, W. *Biochim. Biophys. Acta* **2001**, *1526*, 61−69.
(23) Vermeer, A. W. P.; Bremer, M. G. E. G.; Norde, W. *Biochim. Biophys. Acta* **1998**, *1425*, 1−12.
(24) Kidoaki, S., Matsuda, T. *Langmuir* **1999**, *15*, 7639−7646.
(25) Grabbe, E. S. *Langmuir* **1993**, *9*, 1574−1581.
(26) Lin, J. N.; Brake, B.; Lea, A. S.; Hansma, P. K.; Andrade, J. D. *Langmuir* **1990**, *6*, 509−511.
(27) Moulin, A. M.; O'Shea, S. J.; Badley, R. A.; Doyle, P.; Welland, M. E. *Langmuir* **1999**, *15*, 8776−8779.
(28) Song, D.; Forciniti, D. *J. Colloid Interface Sci.* **2000**, *221*, 25−37.
(29) Zhou, J.; Chen, S. F.; Jiang, S. Y. *Langmuir* **2003**, *19*, 3472−3478.
(30) Kamyshny, A.; Magdassi, S. *Colloids Surf., B* **1997**, *9*, 147−155.

as surface coverage, thickness, and conformation changes. One should mention that, due to the diversity in the reported experimental parameters, such as pH,[28] ionic concentration,[3] and IgG type[14,15] used in previous studies, a direct comparison of experimental results obtained by different measurement methods seems unrealistic. The combination of different in situ measurement techniques would provide a new opportunity to obtain complementary information about the protein adsorption process occurring at the same measurement time and under the same experimental conditions. So far, only a few multitechnique studies have been reported.[31,32−35]

In this study, the adsorption behavior of human immunoglobin G is investigated in a broad solution concentration range (from 100 ng/mL to 3 mg/mL) on a hydrophobic surface by means of (i) quartz crystal microbalance dissipation (QCM-D), (ii) combined surface plasmon resonance (SPR) and Love mode surface acoustic wave (SAW), and (iii) combined QCM-D and atomic force microscopy (AFM) techniques. Among these, both the QCM-D and SAW techniques are based on acoustic probing of the protein layer under investigation, providing information about mass uptake on the sensor. The QCM-D technique also provides a unique set of information about viscoelastic property of the protein layer as a result of complex modeling of the interaction of the acoustic wave with the protein layer and the solvent,[19,20,36,37] while the SAW signal is not sensitive to viscoelastic effects.[38] The viscoelastic variation of the adsorbed protein layer was quantified by comparison of the results from QCM-D and SAW. SPR is an optical method, which provides information about absorbed protein amount and layer thickness.[11,12,31] In addition, information about the water content and thickness of the adsorbed protein layer was deduced from combined SPR/SAW investigation. The water content of the protein film was extracted as both techniques provide information on one common parameter, the thickness of the layer. In a simultaneous measurement, SAW gives information about the density parameter of the film, while SPR gives information about the optical index parameter of the layer. Upon reducing the number of parameters by assuming that both density and optical index scale linearly with the protein/water ratio in the protein layer, one could extract a unique pair of layer thickness and water content values from the simultaneous set of measurements.[39] Moreover, the ambiguous quantitative information deduced from the QCM-D measurement, in terms of adsorbed protein amount,[40−43] was precised using the additional information obtained from the combined SPR/SAW measurements. Finally, AFM is one of the most useful techniques to characterize the organization of the adsorbed protein film scaling down to a molecular resolution;[24,26,27] the combined QCM-D/AFM measurement provides substantial new results, such as adsorption kinetics, lateral film organization, and time-resolved information about the conformation change at the interface.[44,45,46]

The combination of different surface-sensitive techniques allowed us to obtain both adsorption kinetics and structural information, which demonstrates that the results deduced from the various measurements not only validate but also complement each other.

Experimental Section

Materials and Preparation of the Sensor Chip Surfaces. Human immunoglobulin G (chrompure) was purchased from Jacksson ImmunoResearch Inc. 1-Octadecanethiol (ODT) (>97%) was obtained from Aldrich. Ultrapure absolute ethanol was purchased from Riedel-de Haën. The inorganic salts were of pa grade (Merck or Fluka). The buffer solution (PBS, pH = 7.4) was prepared with NaCl (0.15 M) and 1×10^{-2} M Na_2HPO_4/KH_2PO_4. Glycine hydrochloride was from Sigma. The water was of an ultrapure grade for microelectronic purposes ($\Omega < 18$).

QCM-D sensor chips were purchased from Q-Sense-AB (Göteborg, Sweden). The chip is a disc-shaped AT-cut crystal with gold electrodes on both sides. The thickness of the quartz crystal was 330 μm according to the supplier. Before use, the chips were cleaned first with a piranha solution (H_2SO_4/H_2O_2, 7:3 (v/v)), followed by a UV−ozone treatment. The cleaned chips were rinsed with absolute ethanol and immediately immersed into ODT solution (ODT dissolved in ethanol with concentration 10^{-3} M) for 6 h. After SAM formation, the QCM sensor chips were rinsed with ethanol and dried with nitrogen.

Methods and Instrumentation. Experimental Procedures. The experimental procedure for QCM-D tests included (Figure 1) the following: (i) degassed PBS solution injected at time t_0 to get a baseline; (ii) injection of a protein solution with known bulk concentration ($C_{protein}$) at time t_1 with the adsorption kinetics typically followed on-line during 1 h; (iii) injection of PBS solution at time t_2 and 5-times exchange of the chamber volume to remove the protein substance that was not surface confined; (iv) injection of rinsing solution (10 mM glycine−hydrochloride, pH 2.2) at time t_3; (v) additional rinsing step in PBS at time t_4. During the measurement, each time injection introduces a fixed volume solution (3 mL). The flow is stopped after each injection. The combined SPR/SAW measurements were performed by following an analogous injection procedure as the QCM-D experiments.

QCM-D Technique. A commercial QCM-D apparatus (Q-Sense AB, Göteborg, Sweden) was used to simultaneously measure the changes in the resonance frequency (Δf) and in the energy dissipation (ΔD) due to the protein adsorption process. The QCM chip is excited to oscillate in the thickness-shear mode at its fundamental resonance frequency (f_1= 5 MHz) and odd overtones (n = 3, 5, 7) by applying a rf voltage across the electrodes. The measurements are effected by periodically disconnecting the oscillating crystal from the circuit in a computer-controlled way.[43,47] The Q-Sense software determines the resonance frequency and the decay time, τ_0, of the exponentially damped sinusoidal voltage signal over the crystal caused

(31) Caruso, F.; Furlong, D. E.; Kingshott, P. *J. Colloid Interface Sci.* **1997**, *186*, 129−140.
(32) Ortega-Vinuesa, J. L.; Tengvall, P.; Lundström, I. *J. Colloid Interface Sci.* **1998**, *207*, 228−239.
(33) Stadler, H.; Mondon, M.; Ziegler, C. *Anal. Bioanal. Chem.* **2003**, *375*, 53−61.
(34) Caruso, F.; Furlong, D. N.; Ariga, K.; Ichinose, I.; Kunitake, T. *Langmuir* **1998**, *14*, 4559−4565.
(35) Höök, F.; Vörös, J.; Rodahl, M.; Kurrat, R.; Böni, P.; Ramsden, J. J.; Textor, M.; Spencer, N. D.; Tengvall, P.; Gold, J.; Kasemo, B. *Colloids and Surf, B* **2002**, *24*, 155−170.
(36) Höök, F.; Rodahl, M.; Brzezinski, P.; Kasemo, B. *Langmuir* **1998**, *14*, 729−734.
(37) Höök, F.; Rodahl, M.; Keller, C.; Glasmaster, K.; Fredriksson, C.; Dahlqvist, P.; Kasemo, B. *Jt. Meet. EFTF-EEE IFCS* **1999**, 966−972.
(38) Friedt, J. M.; Francis, L.; Choi, K. H.; Campitelli, A. *J. Vac. Sci. Technol., A* **2003**, *21*, 1500−1505.
(39) Friedt, J. M.; Francis, L.; Reekmans, G.; Palma, R. D.; Campitelli, A.; Sleytr, U. B. *J. Appl. Phys.* **2004**, *95* (4), 1677−1680.
(40) Voinova, M. V.; Jonson, M.; Kasemo, B. *Biosens. Bioelectron.* **2002**, *17*, 835−841.
(41) Voinova, M. V.; Rodahl, M.; Jonson, M.; Kasemo, B. *Phys. Scr.* **1999**, *59*, 391−396.
(42) Janshoff, A.; Galla, H. J.; Steinem, C. *Angew. Chem., Int. Ed.* **2000**, *39*, 4004−4032.
(43) Rodahl, M.; Kasemo, B. *Sens. Actuators, A* **1996**, *54*, 448−456.
(44) Choi, K. H.; Friedt, J. M.; Frederix, F.; Campitelli, A.; Borghs, G. *Appl. Phys. Lett.* **2002**, *81* (7), 1−3.
(45) Choi, K. H.; Friedt, J. M.; Laureyn, W.; Frederix, F.; Campitelli, A.; Borghs, G. *J. Vac. Sci. Technol., B* **2003**, *21* (4), 1433−1436.
(46) Friedt, J. M.; Choi, K. H.; Francis, L.; Campitelli, A. *Jpn. J. Appl. Phys.* **2002**, *41*, 3974−3977.
(47) Rodahl, M.; Kasemo, B. *Sens. Actuators, B* **1996**, *37*, 111−116.

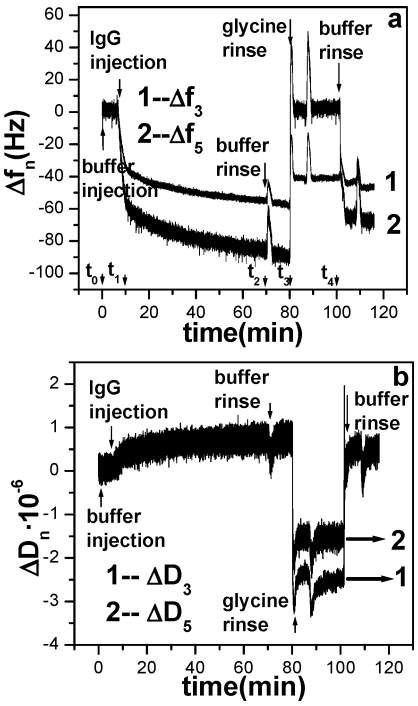

Figure 1. Typical QCM-D experiment for the real-time acquisition of (a) frequency shifts Δf and (b) dissipation changes ΔD induced by protein adsorption on a hydrophobized sensor chip surface. The presented sensograms correspond to the third and fifth overtone frequencies $f_3 = 15$ MHz (curve no. 1) and $f_5 = 25$ MHz (curve no. 2) of the QCM-D device and a bulk solution concentration of human IgG equal to 11.5 μg/mL. The arrows indicate the times for injection of buffer (t_0), protein sample (t_1), and rinsing solutions (t_2, t_3, t_4). (Artifacts due to the exchange of the liquid phase in the measurement chamber are seen as peaks around 70, 80, 88, and 110 min.)

by switching of the voltage applied to the piezoelectric oscillator. This allows to acquire the dissipation factor, D, via the relation

$$D = \frac{1}{\pi f \tau_0} = \frac{2}{\omega \tau_0}$$

where f is the resonance frequency and τ_0 is the relaxation time constant.[37] This energy dissipation, D, is the inverse of the quality factor, Q, which is defined as the center resonance frequency divided by the width-at-half-height of the resonance peak.

Classically, the Sauerbrey relationship has been used for quantitative determination of mass deposited on the sensor surface,[35,36]

$$-\Delta f_{\text{Sauerbrey}} = \frac{1}{nC} m_f = \frac{1}{nC} \rho_f h_f \qquad (1)$$

where the mass sensitivity constant, C, is equal to 17.7 ng/(cm^2·Hz) at $f_0 = 5$ MHz. The Sauerbrey equation has in fact been derived for uniform ultrathin rigid films with material properties indistinguishable from those of the crystal resonator (for instance metallic films deposited onto the gold electrode in a vacuum).[42] Ward,[48] Rodahl and Kasemo,[43,47] and Kankare[49] have demonstrated that for applications in liquid phase the Sauerbrey equation is no longer valid and needs to be corrected for the influence of the medium and the viscoelasticity. Viscoelastic changes in the deposited overlayer on the sensor surface, and entrapment of liquid in rough and porous interfacial structures, create additional frequency shifts besides the ones due to the mass load on the electrode surface.[36,37,42]

Combined QCM-D/AFM Technique. The instrumental setup for the combined QCM-D/AFM technique has been described previously.[46] It included a laboratory-made QCM resonator and a tapping mode scanning force microscope PicoSPM (version 4.19, Molecular Imaging Co.). A tapping-mode cantilever with a spring constant 1.2−3.5 N/m was employed. Nanosensors tips were purchased from ScienTec. The AFM cantilever resonance frequency in the experiments was in the 27.9−30.7 kHz range. Images were acquired over scan areas (2 × 2) and (1 × 1) μm^2 using a S-type piezo scanner.

Combined SPR/SAW Technique. Detail information about the set up for the combined SPR/SAW technique can be found in a recent publication.[39] A modified Ibis II SPR instrument (IBIS Technologies BV) is used to irradiate a 670 nm laser on a quartz substrate and monitor the reflected intensity vs angle with an accuracy of ±2.555°/200 pixels. The ST-cut quartz substrate is patterned with double-finger interdigitated electrode for launching a Love mode acoustic wave at a frequency of 123.5 MHz. The guiding layer is made of a 1.13 μm thick PECVD silicon dioxide layer. The phase and insertion loss of the acoustic wave device are monitored using an HP 4396A network analyzer. The SPR angle shift data are modeled following the formalism previously[39] (and references therein), assuming an optical index of a pure protein to be in the 1.450−1.465 range and the density of a pure protein film to be at most 1.4 g/m^3. The SAW phase shift is converted to a frequency shift by using the locally linear phase to frequency relationship and is then translated into a bound mass using the equation[39]

$$\Delta m/A = \Delta f/(S f_0) \qquad (2)$$

where f_0 is the frequency at which the phase is monitored in an open-loop configuration (123.5 MHz in our case), Δf is the frequency converted from the measured phase, and S is the mass sensitivity calibrated by copper electrodeposition.[38] The method for thickness determination and the quantification of water content in protein layer using combined SPR/SAW measurement has been described previously.[39]

Results and Discussion

Part I: QCM-D and Combined SPR/SAW Measurements. Protein Adsorption Kinetics. The adsorption kinetics of hIgG was investigated in a broad concentration range (from 80.5 ng/mL to 2.3 mg/mL) using the QCM-D method. The adsorption of hIgG at the solid/liquid interface was monitored in real time by measuring the decrease of the resonance frequency (Δf) and the time dependence of the dissipation change (ΔD) (Figure 1).

The adsorption of hIgG on the hydrophobic surface appeared to be irreversible, as is observed from the limited desorption degree after intensive buffer rinsing steps.

In the reminder of this report, the acquired Δf_n and ΔD_n for each overtone n ($n = 3, 5$) will be plotted as quantities after subtraction of the initial baseline signals: $\Delta f_n = f - f t_1$ and $\Delta D_n = D - D t_1$. The experimental data reported in this work refer to the third ($f_3 = 15$ MHz) and fifth ($f_5 = 25$ MHz) overtones. Figure 2a shows the adsorption kinetics of hIgG at the solid/liquid interface for selected solution concentrations. The adsorption kinetics showed an essential dependence on the hIgG concentration.

Despite being based on different detection principles, both the SPR and SAW measurements provided synchronous information on the adsorption kinetics (Figure 3).

However, the combined SPR/SAW measurements did not provide the same kinetic trend as the QCM-D results presented above, which is probably due to the viscoelastic variations that are involved in the frequency shift change in the QCM-D measurement. As shown in Figure 2b, plateau values of the dissipation factor change, ΔD, were not reached within 60 min from the onset of the adsorption at bulk hIgG concentration higher than 115 μg/mL. This suggests that the protein layers might undergo a continu-

(48) Ward, M. D.; Buttry, D. *Science* **1990**, *249*, 1000−1007.
(49) Kankare, J. *Langmuir* **2002**, *18*, 7092−7094.

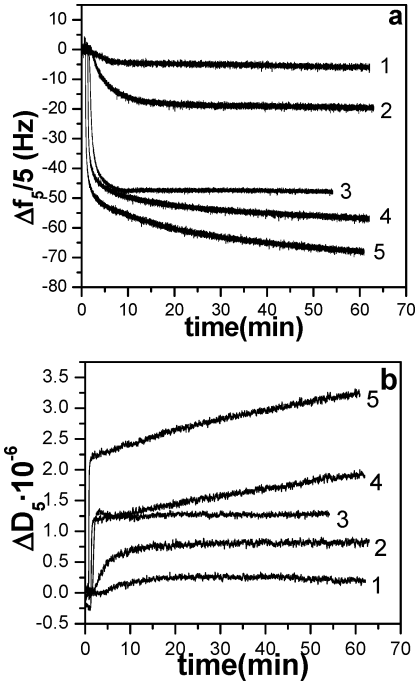

Figure 2. Adsorption kinetics of human IgG monitored as (a) frequency shift Δf and (b) dissipation change ΔD responses versus time at $f_5 = 25$ MHz. The frequency shifts in (a) are presented as normalized quantities $\Delta f_n/n$ ($n = 5$). The protein bulk solution concentrations are 805 ng/mL (1), 11.5 μg/mL (2), 115 μg/mL (3), 0.46 mg/mL (4), and 2.3 mg/mL (5).

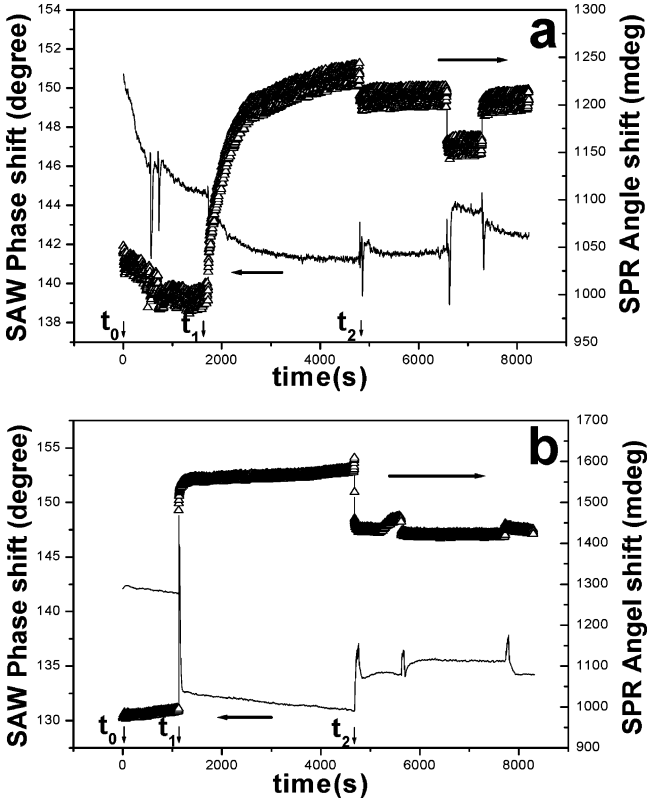

Figure 3. Adsorption kinetics of human IgG measured by a combined SPR and SAW technique for bulk concentrations of (a) 11.5 μg/mL and (b) 2.3 mg/mL. The SAW phase shift is displayed as a thin line while the relative SPR angle shift is displayed as triangles (the scale for SPR is displayed in the right y axis). The arrows on the x axis indicate the following: t_0, PBS injection; t_1, hIgG injection; t_2, buffer rinse.

ous interfacial reorganization at the solid/liquid interface, which results in the viscoelastic variations in the protein layer.

Viscoelastic Variation in the Adsorbed hIgG Layer. In an attempt to detect the viscoelastic variation, which contribute to the measured frequency shifts during the QCM-D measurement, we normalized the plots Δf_n versus time obtained at $n = 3$ and $n = 5$ by the overtone number (procedure recommended by Hook et al.[50]). As a result, we found that the $\Delta f_3/3$ values are generally not identical with the $\Delta f_5/5$ values, differing from the prediction of eq 1. A nonlinear response of the sensor device implies a dominating contribution of viscoelastic variations during the adsorption of the protein layers. The obtained QCM-D responses in this work were classified into two categories: (1) where the normalized $\Delta f_n/n$ curves coincide ($\Delta f_3/3 \equiv \Delta f_5/5$) when the hIgG concentration was lower than 115 μg/mL; (2) where they quantitatively diverge ($\Delta f_3/3 \neq \Delta f_5/5$) when the HIgG concentration was higher than 115 μg/mL (Figure 4).

As shown earlier,[51,52] a strong viscoelastic change during QCM-D measurements in viscous liquids could be confirmed by the overtone scaling law ($\Delta f_n/n^{1/2} =$ constant) (as opposed to the rule ($\Delta f_n/n =$constant) for a rigid deposit). Figure 4b shows that when the bulk hIgG concentration is higher than 115 μg/mL, neither the ($\Delta f_n/n =$constant) rule is applicable nor the scaling law ($\Delta f_n/n^{1/2} =$ constant) is applicable to the Δf_3 and Δf_5 data. However, the discrepancy between the scaled $\Delta f_3/3$ and $\Delta f_5/5$ appears to be much smaller than that between the scaled $\Delta f_3/3^{1/2}$ and $\Delta f_5/5^{1/2}$ quantities for all the investigated hIgG concentrations. This indicates that the mechanical properties of the adsorbed hIgG layer do not resemble those of a rigid layer in the sense of the Sauerbrey equation and that they differ also from those of a viscous liquid in a contact with the sensor surface.

More information about the viscoelastic variations in the hIgG layer contributing to the frequency shift of the QCM-D was obtained from a comparison of the QCM-D and SAW data. The SAW technique measures the mass uptake including trapped water on the sensor surface.[38] The surface coverage represented by the surface mass density, Δm_{SAW}, deduced from the SAW measurements reflects the real mass uptake on the sensor surface. On the other hand, the apparent surface coverage (Δm_{QCM-D}) deduced from the QCM-D frequency shift using eq 1 includes a contribution associated with the viscoelastic variations in the protein layer. Simple conversion of the frequency shift to a surface mass density using eq 1 may lead to an overestimation of the surface deposited mass using the QCM-D method. The viscoelastic effect was quantified by comparison of the surface mass densities Δm_{SAW} and Δm_{QCM-D} (Table 1). Table 1 shows that there is a correlation between the increase of the dissipation factor change ΔD_5 and the surface mass density difference ($\Delta m_{QCM-D} - \Delta m_{SAW}$), observed upon the increase of the hIgG solution concentration.

At hIgG concentration lower than 115 μg/mL, for which the scaling law ($\Delta f_n/n =$ constant) is applicable, the QCM-D measurement overestimates the real mass uptake by about 20%. This indicates a negligible viscoelastic variation in the protein layer formed at low concentrations. At hIgG concentration higher than 115 μg/mL, for which

(50) Höök, F.; Kasemo, B.; Nylander, T.; Fant, C.; Sott, K.; Elwing, H. *Anal. Chem.* **2001**, *73*, 5796−5804.

(51) Friedt, J. M.; Choi, K. H.; Frederix, F.; Campitelli, A. *J. Electrochem. Soc.* **2003**, *150* (10), H229−H234.

(52) Fawcett, N. C.; Craven, R. D.; Zhang, P.; Evans, J. A. *Anal. Chem.* **1998**, *70* (14), 2876−2880.

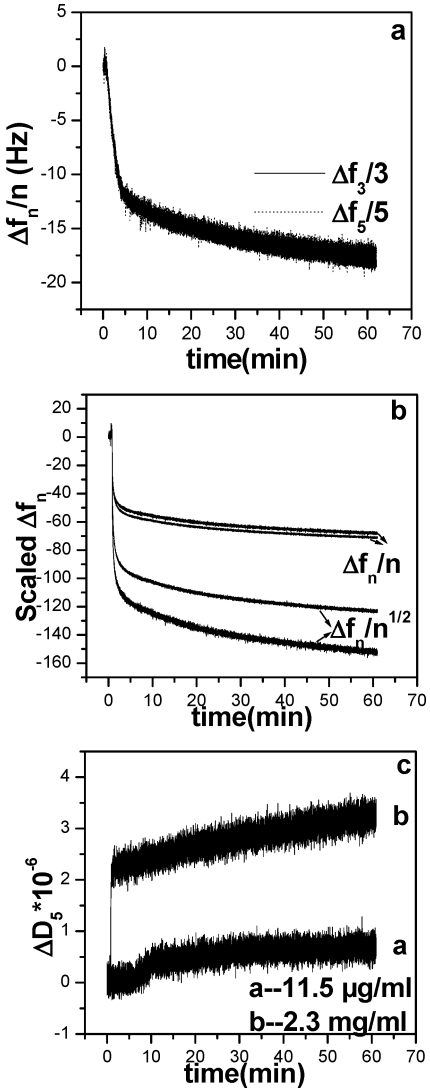

Figure 4. Normalized frequency shifts, $\Delta f_n/n$, versus time obtained for human IgG adsorption at third ($n = 3$) and fifth ($n = 5$) overtones. Two experimental situations are discriminated: (a) The $\Delta f_3/3$ and $\Delta f_5/5$ magnitudes overlap when the bulk hIgG concentration is lower than 115 μg/mL (the IgG solution concentration is 11.5 μg/mL in this example and $\Delta D_{5(t=60\ \mathrm{min})} = 0.62 \times 10^{-6}$). (b) The $\Delta f_3/3$ and $\Delta f_5/5$ curves are divergent when the bulk hIgG concentration higher than 115 μg/mL (the solution concentration of IgG is equal to 2.3 mg/mL in the presented example and $\Delta D_{5(t=60\ \mathrm{min})} = 3.14 \times 10^{-6}$). The $\Delta f_n/n^{1/2}$ curves for this concentration are also shown in (b). The dissipation kinetics of ΔD_5, corresponding to the two bulk hIgG concentrations in (a) and (b), are shown in (c).

Table 1. Surface Mass Density ($\Delta m_{\mathrm{QCM-d}}$) Deduced from QCM-D Measurements in the 5th Mode, Surface Mass Density (Δm_{SAW}) from Love Mode SAW Measurements, Dissipation Change ΔD_5, and Surface Mass Density Difference ($\Delta m_{\mathrm{QCM-d}} - \Delta m_{\mathrm{SAW}}$) Associated with the Viscoelastic Variation

hIgG concn	$\Delta m_{\mathrm{QCM-D}}$ (ng/cm^2)	Δm_{SAW} (ng/cm^2)	dissipation change ΔD_5 (10^{-6})	$\Delta m_{\mathrm{QCM-D}} - \Delta m_{\mathrm{SAW}}$ (ng/cm^2)	ratio of $\Delta m_{\mathrm{QCM-D}}$ to Δm_{SAW}
11.5 μg/mL	361 ± 24	300 ± 50	0.62	60	1.2
57.5 μg/mL	531 ± 53	410 ± 55	1.26	121	1.3
115 μg/mL	726 ± 53	475 ± 60	1.34	251	1.5
0.46 mg/mL	977 ± 60	609 ± 70	2.10	368	1.6
1.38 mg/mL	1168 ± 62	740 ± 50	2.89	428	1.6
2.3 mg/mL	1340 ± 55	850 ± 50	3.15	490	1.6

the scaling law ($\Delta f_n/n$ = constant) is not applicable, the QCM-D measurement overestimates the real mass uptake by over 50%, which indicates a substantial viscoelastic vatiation in protein layer formed at high concentration.

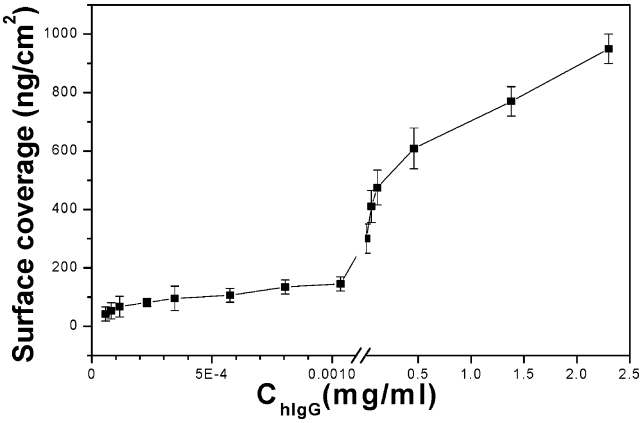

Figure 5. Surface mass density as a function of the bulk concentration of human IgG. For protein concentrations lower than 11.5 μg/mL, the surface coverage is deduced from QCM-D measurements; for protein concentrations equal or larger than 11.5 μg/mL, the surface coverage is determined by love mode SAW measurements. The adsorption isotherm refers to 1 h adsorption time at temperature 21 °C.

Monolayer and Supramonolayer Regimes: Deduced from Surface Mass Density. The adsorption isotherm, corresponding to the surface coverage of hIgG on the sensor surface as a function of its concentration in solution, is presented in Figure 5. As we discussed above, when the bulk hIgG concentration ranges from 80.5 ng/mL to 11.5 μg/mL, the surface mass density value, $\Delta m_{\mathrm{QCM-D}}$, determined from the QCM-D test and eq 1 will not overestimate the real surface mass density because of the negligible viscoelastic variation. Thus, for these concentrations, the surface coverage value was obtained from QCM-D data and eq 1. On the other hand, the surface coverage for bulk concentrations above 11.5 μg/mL was determined by SAW measurements and eq 2 because the QCM-D measurement overestimates the real mass uptake when the viscoelastic variation is significant.

The surface coverage exhibits a nonlinear dependence on the protein solution concentration, C_{hIgG}, which was varied in the present study in an extended interval from 80.5 ng/mL to 2.3 mg/mL. The shape of the obtained adsorption isotherm differs remarkably from a typical adsorption curve terminated by a saturation plateau that corresponds to fully occupied adsorption sites upon monolayer formation at the interface.[22] The surface coverage value of 609 ng/cm^2, obtained at a hIgG concentration of 0.46 mg/mL, is much larger than the highest possible surface coverage values for IgG monolayer. A densely packed IgG monolayer would give a surface coverage ranging from 200 to 550 ng/cm^2,[3] depending on the orientation of the absorbed IgG molecules.

On the basis of the obtained surface coverage values, the adsorption isotherm of hIgG is interpreted in terms of the surface packing density, which varies from submonolayer to a monolayer one and subsequently reaches a multilayer configuration upon the increase of C_{hIgG}.

In other studies, it has been reported that IgG adsorption on hydrophobic surfaces leads to a plateau value of the surface coverage corresponding to a monolayer packing when the bulk IgG concentration is high.[3,21] Few reports have described a double layer formation upon IgG adsorption on hydrophobic surfaces.[13,25,28] In this study, the hIgG adsorption did not saturate at a monolayer level. In contrast, it resulted in supramolecular structures and

Table 2. Water Content and Layer Thickness of the Adsorbed HIgG Layer Determined after 1 h of Adsorption onto Hydrophobic Sensor Surfaces

hIgG concn	water content (%)	film thickness (nm)
11.5 μg/mL	0 ± 10	2.3 ± 0.3
57.5 μg/mL	0 ± 10	3.5 ± 0.5
115 μg/mL	0 ± 10	3.5 ± 0.3
0.46 mg/mL	0 ± 10	4.6 ± 0.7
1.38 mg/mL	0 ± 10	6.0 ± 0.2
2.3 mg/mL	0 ± 10	7.2 ± 0.6

did not reach a plateau value within the bulk concentration range investigated in this paper. The surface coverage values in our measurements indicated that the bulk hIgG concentration which leads to a full monolayer is equal to or slightly above 11.5 μg/mL. This concentration range is in agreement with those reported previously.[6,7,22]

To identify the lowest possible concentration that is able to form a fully covered monolayer on the hydrophobic surface, additional QCM-D experiments were performed. Three different surfaces preabsorbed with hIgG at bulk concentrations of 805 ng/mL, 11.5 μg/mL, and 57.5 μg/mL were exposed to aqueous solution of 200 μg/mL bovine serum albumin (BSA) for 30 min. The incubation with BSA resulted in frequency shifts of 40, 17, and 0 Hz, respectively, in the fifth overtone. This strongly indicates that the hydrophobic surface is nearly fully covered by a hIgG film when the bulk hIgG concentration reaches a value higher than 11.5 μg/mL. When the hIgG concentration increases above 11.5 μg/mL, the corresponding surface mass density is higher than 300 ng/cm^2. This surface coverage value is within the range of the theoretical monolayer coverage (200 ng/cm^2 for IgG monolayer in a "flat-on" orientation and 370 ng/cm^2 for IgG monolayer with "end-on" orientation[3]).

Water Content of the Adsorbed hIgG Film. This study quantitatively determined the water content in the adsorbed IgG layer by means of combined SPR/SAW measurements. The employed QCM and SAW techniques, which are based on acoustic probing of the protein layers under investigation, measure the combined mass uptake coming from both the adsorbed protein and trapped water in the protein layer.[35,50] On the other hand, the mass uptake deduced from optical or labeling techniques does not include the mass of trapped water. Thus, the comparison between QCM and optical techniques could be used to demonstrate the presence of hydrodynamically coupled water in deposited protein layer.[31,35,54,55] However, it is known that the viscoelastic variations in the adsorbed protein layers also contribute to the frequency shift in a QCM measurement.[40−42] Therefore, direct comparison of the mass uptake values deduced from QCM and optical technique overestimates the real mass value of trapped water because of the viscoelastic variations detected by QCM measurement.

To be able to precisely extract the water content of the adsorbed hIgG layer, we explore the fact that the SAW signal has been shown not to be sensitive to the hydrodynamic drag[38] in protein layers. Using experimental data as those shown in Figure 3 and using the fitting procedure described in ref 39, we determined the water content and the thickness of hIgG films adsorbed at different solution concentrations. The results are presented in Table 2. We found that the hIgG layer, formed after 1 h of adsorption from solutions with various concentrations of hIgG, barely contains trapped water, under the assumption that the optical index is in the 1.450−1.465 range and the density of the pure protein layer is 1.4 g/m^3.[39] The determined film thickness varies from 3 to 7 nm for hIgG concentration increasing from 11.5 μg/mL to 2.3 mg/mL. In other studies, it has been reported that protein layers contain a certain degree of associated water.[35,36,50] The exact amount of trapped water depends on the protein type and the structure of the formed protein layer. It is suggested that the adsorbed IgG tends to change its conformation on the hydrophobic surface to achieve its most favorable surface interaction and energy state.[8,14] In this study, it is likely that most of the trapped water is getting expelled from the films upon durable contact with the solid support because of the hydrophobic interaction between the protein macromolecules and the hydrophobic surface. The effective protein film thickness (Table 1), determined here from combined SPR/SAW measurements, appears to be smaller than the extended state molecular dimension of the IgG molecule (14 × 10 × 4 nm^3).[3,21,25,34] Conformation changes occurring upon contact with hydrophobic support may explain the resulting small thickness of the protein layers.

Conformation Change and Layer Organization Deduced from QCM-D Results. Generally, the observed changes in the dissipation factor in a QCM-D measurement might be due to conformation changes in the protein layers and/or to the trapped liquid in the layer.[33,36,37,42,56] As the SPR/SAW measurement ruled out the presence of trapped liquid in the investigated hIgG layer, the measured dissipation change ΔD in this study should be due to the conformation changes at the solid/liquid interface.

Using the simultaneously measured Δf_5 versus time and ΔD_5 versus time QCM-D responses (Figure 2), we created ΔD_5 versus Δf_5 plots characterizing the viscoelastic nature of the hIgG layers adsorbed at the solid/liquid interface.[56] Figure 6 presents two types of relationships deduced from such experiments, for which one (Figure 6a) or more than one (Figure 6b,c) slope were discriminated in the generated plots. The different slopes in the $\Delta D-\Delta f$ plots indicate that kinetic processes with diverse relaxation times occur during adsorption. Defining the slope of the plots as K ($K = \Delta D/\Delta f$), one could expect that a rigid and compact layer would yield a small value of K.[56] This was experimentally observed for hIgG concentration of 805 ng/mL (Figure 6a).

The appearance of more than one slope is resolved upon increasing the bulk protein concentration above 11.5 μg/mL. We have demonstrated that above this concentration, the hIgG adsorption results in a monolayer surface coverage. These multiple slopes imply that the interfacial phenomena, which happened at hIgG concentrations higher than 11.5 μg/mL, are associated with multiple adsorption stages.[36,37,56,57] During adsorption, the IgG molecules are involved in direct adhesion onto the hydrophobic surface and in interfacial rearrangement including conformation change.[14,19,22,23,27] For the concentration above 11.5 μg/mL, at which more than one slope in the $\Delta D-\Delta f$ plots is established, we suggest that the initial slope is associated with molecular adsorption rather than with conformation change. This is because that, at higher concentrations, the initial adsorption kinetics is much faster than the conformation change time scale. After the completion of a monolayer coverage, the con-

(53) Gizeli, E. Acoustic transducers. In *Biomolecular Sensors*; Gizeli, E., Lowe, C. R., Eds.; Taylor & Francis: London, 2002.
(54) Muratsugu, M.; Ohta, F.; Miya, Y.; Hosokawa, T.; Kurosawa, S.; Kamo, N.; Ikeda, H. *Anal. Chem.* **1993**, *65*, 2933−2937.
(55) Caruso, F.; Rodda, E.; Furlong, D. N. *J. Colloid Interface Sci.* **1996**, *178*, 104−115.
(56) Rodahl, M.; Höök, F.; Fredriksson, C.; Keller, C. A.; Krozer, A.; Brzezinski, P.; Voinova, M.; Kasemo, B. *Faraday Discuss.* **1997**, *107*, 229−246.
(57) Höök, F.; Rodahl, M.; Kasemo, B.; Brzezinski, P. *Proc. Natl. Acad. Sci. U.S.A.* **1998**, *95*, 12271−12276.

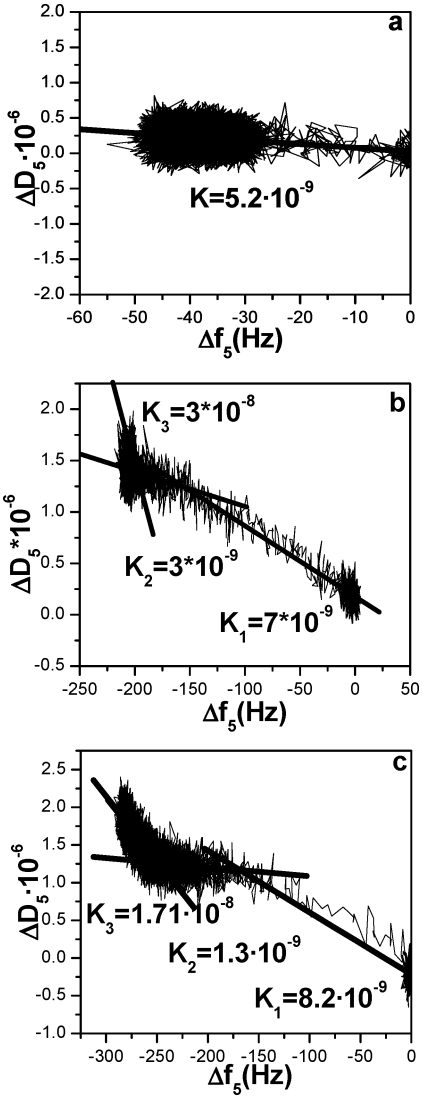

Figure 6. ΔD_5 versus Δf_5 plots generated from experimental data for human IgG adsorption at various solution concentrations. Two categories of relationships with one slope (k_1) or three slopes (k_1, k_2, and k_3) were established upon increasing the bulk protein concentration: (a) one slope (at bulk hIgG concentration 805 ng/mL); (b) three slopes (at bulk hIgG concentration 115 μg/mL); (c) three slopes (at bulk hIgG concentration 0.46 mg/mL).

Table 3. Slopes in the $\Delta D-\Delta f$ Plots from Figure 6 (K_i = Slope Determined from $\Delta D/\Delta f$ Curves)

hIgG concn	initial slope K_1 ($\times 10^9$)	second slope K_2 ($\times 10^9$)	third slope K_3 ($\times 10^8$)
805 ng/mL	5	none	none
11.5 μg/mL	7	none	none
57.5 μg/mL	7	none	none
115 μg/mL	7	0.7	3
0.46 mg/mL	8	1	2
2.3 mg/mL	13	2	1.2

formation change becomes dominant. Thus, a second slope is resolved because of such a conformation change. Under all investigated conditions, the second slope is essentially smaller than the first one (Table 3). It is indicative of the formation of a compact film. In addition, we identified "the break points" in the $\Delta D-\Delta f$ plots, at which alteration to the different slopes K_i occurs. Figure 6 demonstrates that all first break points in the $\Delta D-\Delta f$ plots are close to an absolute Δf_5 value of 150 ± 15 Hz. The conversion of this frequency shift to protein surface coverage gives a surface coverage value ranging from 350 to 390 ng/cm^2. Here, it was considered that QCM-D overestimates the mass uptake by 1.2−1.6, and the mass uptake, i.e., 531 ng/cm^2, deduced from eq 1 was modified by this ratio. The resulting surface coverage value is in a good agreement with the theoretical monolayer coverage, 370 ng/cm^2, when the IgG packing is assumed with an "end-on" orientation.[3] Thus, during the protein adsorption, the first break point in QCM-D data corresponds to a monolayer coverage. This observation further confirms that the initial slope is associated with molecular adsorption and the conformation change becomes dominant after the completion of a monolayer coverage, i.e, first break point.

At bulk hIgG concentrations above 0.46 mg/mL, there is a clear third slope in the $\Delta D-\Delta f$ plots. We have suggested that a multilayer is formed when the hIgG concentration is higher than 0.46 mg/mL. Therefore, the third slope probably corresponds to an additional layer or a thicker layer formation. The third slope is larger than the first and the second slope. They indicate a loosely bound and more flexible layer. Such a loosely bound protein overlayer was indicated also by Höök et al.[56,57] Thus for these concentration higher than 0.46 mg/mL, the adsorption of hIgG first forms a full monolayer, i.e., the first slope, then undergo a conformation change, i.e., the second slope, and finally forms a second overlayer, i.e., the third slope.

For the concentrations lower than 11.5 μg/mL, at which the $\Delta D-\Delta f$ plots display only one slope, we assume that hIgG molecular adsorption and its conformation change occur simultaneously or at the same time scale.

The QCM-D data in this study suggest a conformation change happens during the hIgG adsorption. Höök et al.[56,57] also envisaged conformation changes in adsorbed protein monolayers. It has been known that protein molecules tend to spread, once adsorbed on a hydrophobic surface, to maximize the interaction with the surface.[8,14,22,23,25,27] The effective layer thickness determined in this study supports the shrinking of the protein layer due to such conformation changes (Table 2). Previous AFM investigations have supported a "flattening" effect in the protein monolayer thickness because of the conformation changes.[27,58]

We have demonstrated that a full monolayer will form when the bulk hIgG concentration is higher than 11.5 μg/mL. The surface coverage value for 57.5 μg/mL hIgG adsorption is around 400 ng/cm^2, which is close to the theoretical monolayer coverage, i.e., 370 ng/cm^2, with an "end-on" IgG orientation.[3] On the basis of the surface coverage value in this study, we suggest that an "end-on" orientation exists in the formed hIgG monolayer. It has been known that IgG prefers an "end-on" interfacial orientation with its Fc domain contacting the hydrophobic surface.[14−16,21,28,30] The Fc part of IgG is more hydrophobic than the F(ab) part.[30,59] It has been shown that the Fc part has lower structure stability.[14,60] Hence, these molecular properties promote the adsorption of IgG molecules with their Fc parts onto the surface, which directs the F(ab) portion toward the aqueous solution.

Part II: Combined QCM-D/AFM Measurement. By using combined QCM-D/AFM measurement, the protein adsorption behavior was monitored on both macroscopic and microscopic scale simultaneously.[44,45,46] Because the protein adsorption may depend on the roughness of the

(58) Bergkvist, M.; Carlsson, J.; Karlsson, T.; Oscarsson, S. *J. Colloid Interface Sci.* **1998**, *206*, 475−481.
(59) Kamyshny, A.; Toledano, O.; Magdassi, S. *Colloids Surf., B* **1999**, *13*, 187−194.
(60) Buijs, J.; White, D. D.; Norde, W. *Colloids Surf., B* **1997**, *8*, 239−249.

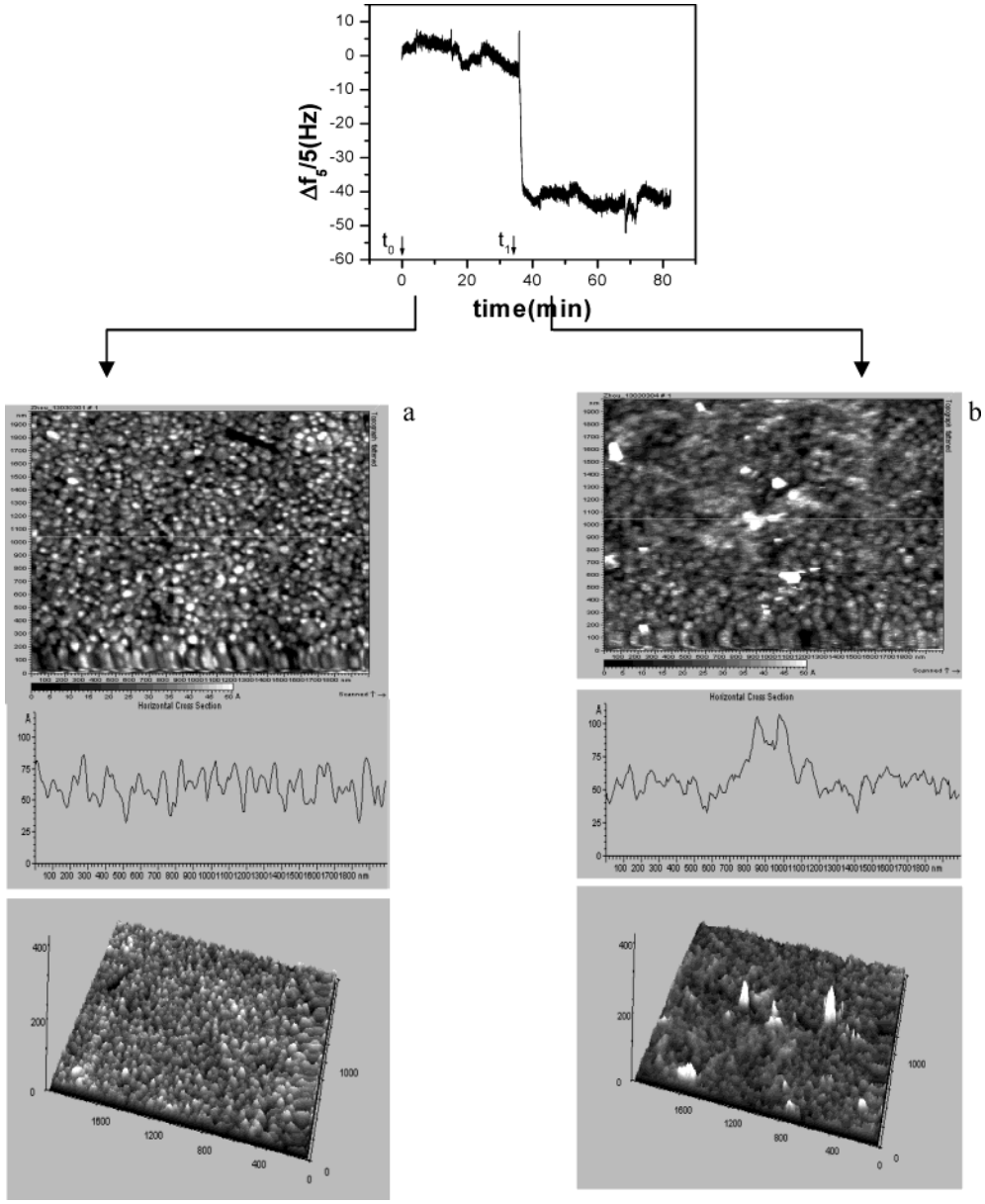

Figure 7. Simultaneous in situ investigation of the human IgG adsorption process at a bulk hIgG concentration of 115 μg/mL by combined tapping-mode atomic force microscopy and quartz crystal microbalance (AFM-QCM) measurements in liquid medium. The QCM response is presented as a normalized frequency shift, $\Delta f_n/n$, recorded at the fifth mode ($f_5 = 25$ MHz). Times t_0 and t_1 indicate the instants of injection of the aqueous buffer and the IgG solution, respectively. The large arrows indicate the time spots from the sensogram at which the scanning of the microscopic images begins: (a) bare sensor chip surface in aqueous buffer; (b) domain surface morphology after adsorption of IgG (the cross section indicates a 3D island growth and heterogeneous interfacial distribution of IgG). The image size is (2×2) μm^2.

surface,[61] to be able to compare the combined QCM/AFM results with the above QCM-D and SPR/SAW results, we investigated hydrophobized gold surfaces bearing the same roughness in all measurements. AFM investigation showed that the morphological features of the sensor chips remained unaltered upon the chemisorption of a self-assembed alkane thiol monolayer. Gold granules with diameters around 50−150 nm were present, and they exhibited height differences of maximum 5−7 nm. The root-mean-square (rms) roughness value evaluated by AFM investigations of several bare QCM chips was in 3−5 nm range.

Protein Surface Coverage. Figure 7 shows combined QCM/AFM experiments displaying (i) the variation of the normalized resonance frequency $\Delta f_5/5$ during the adsorption process and (ii) the on-line AFM images obtained simultaneously with the QCM sensogram in liquid medium. The morphology of the hydrophobized sensor chip equilibrated with buffer solution before the injection of the protein (i.e. during the baseline acquisition, $\Delta f = 0$ Hz) is presented in image a.

The adsorption of hIgG for a bulk concentration of 805 ng/mL was detected by the QCM sensor with a frequency shift of $\Delta f_5/5 = 10$ Hz. However, the AFM image did not reveal an apparent morphology change of the initial chip surface, which remained to be of a granular type (image not shown). Comparing the dimensions of the IgG molecule ($14 \times 10 \times 4$ nm^3)[3,21,25,34] with those of the gold granules (diameters around 50−150 nm), one could suggest that individual IgG molecule should be imaged by AFM on flat terraces. However, individual hIgG

(61) Denis, F. A.; Hanarp, P.; Sutherland, D. S.; Gold, J.; Mustin, C.; Rouxhet, P. G.; Dufrêne. *Langmuir* **2002**, *18*, 819−828a.

molecules could not be resolved here because of the flattening effect during AFM measurement. The latter is caused by both the conformation change and tip convolution effects.[11,26,34] The flattening effect enhances the *x* and *y* dimensions of imaged protein, giving rise to lateral dimensions similar as those of the gold granules. Therefore, it is hard to distinguish the adsorbed protein domains from the gold granules.

The initial rms roughness value for the bare sensor chip is around 2.8 nm. After adsorption of 805 ng/mL hIgG, the rms value remained unaltered. According to the results presented in part I, the surface mass density after the adsorption of 805 ng/mL hIgG is 134 ± 40 ng/cm^2. We estimated that this density only corresponds to 36 ± 9% of a full monolayer coverage (assuming that hIgG adopts an "end-on" orientation, the monolayer coverage would correspond to 370 ng/cm^2). Such a low surface coverage is not expected to alter the morphological characteristics of the initial sensor surface considerably.

Image b in Figure 7 is recorded 15 min after the onset of the hIgG adsorption from a solution concentration of 115 μg/mL. It reveals masking of the gold grains due to substantial protein deposition. The recorded normalized frequency shift is considerable at this hIgG solution concentration ($\Delta f_5/5$ = 45 Hz). The observed smeared morphological surface features in image 7b are indicative of a soft character of the protein layer. As we demonstrated in the previous section, 115 μg/mL hIgG forms a fully covered protein film. Thus, these results indicate that a monolayer film can be distinguished from a submonolayer structure by AFM imaging although the single hIgG molecule could not be clearly detected.

The AFM image obtained for 11.5 μg/mL hIgG adsorption further confirms this observation (image not shown). On the basis of the surface mass density values and the BSA adsorption test, we concluded that the adsorption of 11.5 μg/mL hIgG forms a layer corresponding to 81% surface coverage. However, the difference between the AFM images for adsorption at 805 ng/mL and 11.5 μg/mL was not apparent. In contrast, the difference between the AFM images obtained at 11.5 and 115 μg/mL hIgG adsorption was quite apparent. These results suggest that the AFM image does reflect the degree of surface coverage and this technique is well effective to distinguish fully covered surfaces from partly covered surfaces.

Protein Layer Organization. The AFM imaging technique was further used to resolve the ambiguity in determining the organization of the layer formed upon 115 μg/mL hIgG adsorption in the QCM and SPR/SAW measurements. As we discussed in part I, at least a monolayer is formed for the protein layer formed from 115 μg/mL hIgG adsorption. However, whether only a monolayer or multiplayer structure is existed in this layer could not be determined only by the surface mass density value, i.e., 475 ng/cm^2. Figure 7b shows an apparent island structure protruding above a homogeneous underlayer. Since at least one protein monolayer is formed on the surface, these protruding structures cannot be identified as uncovered gold granules. Thus, the protruding island structures should be adsorbed hIgG domains. The average height difference between the protruding part and the underlayer is 6 nm. With the assumption that the adsorption of 115 μg/mL hIgG leads to the formation of a monolayer structure and the fact that the height difference is 6 nm, the organization of such a assumed monolayer should correspond to a combination of "flat-on" and "end-on" orientations.[3] To explain the observation for the 115 μg/mL IgG adsorption (Figure 7b), most of the hIgG molecules should be present with a "flat-on" orientation (4 nm in height) and a limited fraction of the hIgG should be presented with an "end-on" orientation (10 nm in height). However, the surface coverage for such a layer would not reach a value as high as 475 ng/cm^2. Thus, a monolayer organization with combined "flat-on" and "end-on" orientation is ruled out. Considering the surface coverage value and the AFM image feature (Figure 7b), it is reasonable to suggest that the adsorption of 115 μg/mL hIgG first leads to the formation of a monolayer and that additional IgG molecules adhere on top of the first protein layer to form a second layer with an island structure.

Conclusion

We investigated hIgG adsorption on a hydrophobic surface with emphasis on the kinetic, viscoelatic variation, interfacial hydration, and structural details obtained by QCM-D, combined SPR/SAW, and combined QCM-D/AFM measurement techniques.

The QCM-D and the combined SPR/SAW data show similar trends in the adsorption kinetics. The adsorption of hIgG on a hydrophobic surface is very fast and irreversible. The adsorption kinetics show concentration dependence: the higher the concentration, the faster the initial adsorption stage is. Interestingly, the higher the concentration, the longer the time to reach a saturation of the signal at the solid/liquid interface.

The adsorption isotherm indicates that the hIgG adsorption does not reach a plateau value even when the bulk hIgG concentration is as high as 2.3 mg/mL. The hIgG forms a fully covered monolayer with presumed "end-on" orientation when the concentration is higher than 11.5 μg/mL but does not exceed 57.5 μg/mL. Further increase in the bulk concentration leads to a multilayer like structures. A conformation change occurring after the extended contact of the initial monolayer with the solid surface results in a compact monolayer with a thickness much less than 10 nm.

For the hIgG layer formed at low surface coverage, the QCM signal clearly reveals the protein adsorption, while the AFM imaging cannot resolve the morphology of the layer. For hIgG layer corresponding to a monolayer coverage or above, both the QCM and AFM techniques response to the features of the protein adsorption.

The viscoelastic effect established in QCM-D measurement could be quantified by the comparison of the results from QCM-D and combined SPR/SAW. Considering that the adsorbed hIgG layer barely contains water, as suggested by the combined SPR/SAW measurement, the dissipation changes are attributed to the viscoelastic variation occurring within the protein layer and related to the conformation change of the adsorbed hIgG molecules. The QCM-D slightly overestimates the mass uptake on the sensor surface by a ratio around 1.5. This implies that there is a limited viscoelastic effect in the protein layer as indicated by the small dissipation factor value.

The present investigation covers a broad range of hIgG bulk concentrations (from 87.5 ng/mL to 2.3 mg/mL). It is in agreement with results reported by others previously and also provides new information on the adsorption behavior of hIgG. This study demonstrates the merit and potential of using combined techniques for studying protein adsorption, especially for the elimination of possible quantitative ambiguities resulting from viscoelastic and hydration effects.

Acknowledgment. The corresponding author wishes to thank the IMEC for its financial support of the Ph.D research program.

LA036251D